Research Article

Shear Behavior of Ultra-High-Performance Concrete Shear Pockets with Large-sized Studs in Full-Depth Precast Concrete Bridge Deck under Push-off Tests

Krissachai Sriboonma
Department of Teacher Training in Civil Engineering, Faculty of Technical Education, King Mongkut's University of Technology North Bangkok, Bangkok, Thailand

Nantawat Khomwan*
Department of Civil Engineering, Faculty of Engineering at Kamphaeng Saen, Kasetsart University Kamphaeng Saen Campus, Nakhon Pathom, Thailand

Krit Chaimoon
Structural Engineering Research Unit, Faculty of Engineering, Mahasarakham University, Maha Sarakham, Thailand

Kittipoom Rodsin
Civil and Environmental Engineering Technology, College of Industrial Technology, King Mongkut's University of Technology North Bangkok, Thailand

* Corresponding author. E-mail: fengnwk@ku.ac.th
DOI: 10.14416/j.asep.2025.12.003
Received: 6 July 2025; Revised: 17 September 2025; Accepted: 28 October 2025; Published online: 15 December 2025

Abstract
Full-Depth Precast Concrete (FDPC) bridge deck panel system has been widely used for highway construction due to its rapid construction and replacement process as well as cost effective. This system was used with a cluster of large size headed-stud shear connectors (31.8 mm diameter) for transferring composite actions between concrete decks and steel girders. For more effectiveness in composite actions and cracks controlling around a cluster of large-size studs, Ultra High-Performance Concrete (UHPC) with compressive strength of 120 MPa was utilized for shear pocket connection between the normal strength concrete (NSC) 50 MPa bridge deck panels and steel girders. Eight specimens were push-off evaluated with variable geometries and layouts of shear pockets (9-, 12- and 15-inches width), and variable numbers of clustered large-size studs (4, 6 and 8 studs). The results showed three stages of crack pattern from the flexure, shear, and failure behaviors. Concrete crushing at the FDPC interface propagated across the slab section was observed in all specimens, while the shear plane cut at the UHPC section was found in the specimen with 4 studs. The shear strength at failure was compared to the nominal shear resistance of the design equations, AASHTO LRFD and Eurocode 4, in terms of the failure load ratio. The compatible results were found in the specimens with 4 studs in a square shape pocket, while the others found fewer results from 3.6% to 9.4%. The specimens with more than 4 studs required a reduction factor of 0.8 for each stud pair increment to evaluate a suitable shear resistance capacity for this system.

Keywords: Finite Element, Ultra high-performance concrete, Shear pocket, Full-depth precast concrete, Large-size stud

1 Introduction

The accelerated construction of bridges has become a paramount objective in modern civil engineering, driven by the need to minimize traffic disruption, reduce lifecycle costs, and enhance structural durability. Among the innovative solutions, the Full-Depth Precast Concrete (FDPC) bridge deck panel

system has emerged as a cornerstone of accelerated bridge construction. By prefabricating deck panels and girders off-site, this system ensures superior quality control, rapid assembly, and reduced environmental impact, making it particularly advantageous for urban and rural infrastructure projects [1], [2]. However, the success of such systems hinges critically on the performance of shear connections between precast components, which must reliably transfer interfacial shear forces to ensure composite action and structural integrity.

Traditional shear connectors, such as small-headed studs embedded in normal-strength concrete (NSC), often face limitations in high-shear zones. The dense arrangement of these studs can lead to welding inefficiencies, concrete splitting cracks, and compromised fatigue resistance [3]. To address these challenges, large-sized studs (greater than 30 mm diameter) have been proposed, offering higher shear capacity and reduced numbers per unit length. The study of Badie *et al*., [4] revealed that the full-scale test of the composite bridge deck system with clusters of large-size diameter studs of 31.8 mm (1¼") could extend the spacing of clusters up to 1200 mm (48"). This could effectively transfer the composite actions under the service loading conditions. However, their adoption in NSC is constrained by transverse splitting forces, which induce longitudinal cracks and reduce load-bearing efficiency [5]. This limitation underscores the need for advanced materials capable of harnessing the full potential of large studs. Sriboonma *et al*., [6] explained the practical guideline for using large size stud shear connectors in full-depth precast bridge deck panels to efficiently carry the composite actions and shear transfers.

Ultra-high-performance concrete (UHPC), characterized by compressive strengths exceeding 120 MPa [7] and remarkable tensile ductility due to steel fiber reinforcement, presents a transformative solution. Its dense microstructure and superior bond strength mitigate cracking under high-stress concentrations, making it ideal for shear connections [8], [9]. Recent studies demonstrate that UHPC-embedded studs exhibit 15–20% higher shear strength and stiffness compared to NSC, with negligible concrete damage even at failure [10]. Furthermore, UHPC's durability—resistance to chloride ingress, freeze-thaw cycles, and abrasion—ensures long-term performance in aggressive environments [11]. Its superior mechanical properties also allow for a reduction in shear reinforcement in congested areas [12].

FDPC bridge deck panel systems that employ large clustered studs embedded in UHPC shear pockets have emerged in recent research as a promising approach to improve composite action, constructability, and durability of prefabricated bridge decks. Studies report that filling discrete shear pockets with UHPC substantially increases local shear capacity and stiffness compared with conventional grout or normal-strength concrete pockets, allowing designers to use fewer but larger pockets and grouped studs without compromising load transfer [13], [14]. Clustered large-diameter studs provide higher local load-carrying capacity and improved resistance to shear concentrations (particularly under hogging regions and concentrated transfer zones), enabling more efficient transfer of interface forces between precast deck panels and supporting girders [14], [15]. In practice, this can reduce the number of connector lines required across the deck, simplify field welding/installation operations, and shorten on-site assembly time — advantages that are particularly valuable for accelerated bridge construction projects [13], [15]. UHPC pockets also limit cracking and local damage around the pocket region, improving serviceability and long-term durability in highly stressed zones when compared to ordinary pocket grouts [14], [16]. Recent full-scale and push-out testing further confirm that properly detailed UHPC pockets with adequate confinement or reinforcing can achieve reliable ductile behavior and system-level composite action, like or better than traditionally cast-in-place decks [16], [17].

Despite these advantages, the interfacial shear behavior of UHPC in composite systems remains underexplored, particularly for shear pockets—critical zones where precast girders and deck panels interconnect. Conventional pocket designs, relying on plain UHPC infill, may not fully exploit the material's potential under cyclic or extreme loads. To enhance load transfer and ductility, steel L-angle ring confinement is proposed herein. Sriboonma *et al*., [18] assessed the push-off specimens using various types of shear pocket confinement and found that steel L-angle confinement would be the best efficiency confinement, in terms of strength and ductility (load-slip), for a cluster of large-size studs under the NSC slabs. This also included the fatigue loading condition per the test results under cyclic loading. Several push-off tests of a cluster of large size studs with different types of steel confinement were investigated under static and cyclic loading [19]. By encircling shear

pockets with steel angles, lateral confinement pressure is introduced, restricting crack propagation and improving the triaxial stress state around studs. This approach builds on confinement techniques validated in column and joint applications [20], adapting them to shear connections for the first time.

Existing design codes, such as AASHTO LRFD and Eurocode 4, often underestimate the shear capacity of UHPC connections because they are primarily based on NSC-derived models [21], [22]. Recent push-out tests on UHPC-filled pockets demonstrate that current equations do not adequately capture UHPC's distinctive cohesion and dowel action, resulting in overly conservative predictions [9]. Furthermore, the interaction between confined UHPC pockets and large-diameter studs has not been fully quantified, highlighting the need for additional experimental validation. Recent studies also identify several research gaps that must be addressed prior to the standardized adoption of FDPC systems, including issues related to long-term constructability and replacement, fatigue performance under live loading, design provisions for shear pocket dimensions, limitations on the number of studs per pocket, and the effectiveness of different confinement strategies for UHPC pockets.

The present study focuses specifically on the shear behavior of UHPC shear pockets with L-angle ring confinement containing clusters of large-diameter studs, examined through a series of push-off tests. The variables investigated include the pocket dimensions (width and length) of FDPC panels containing stud clusters of 4, 6, and 8 large studs, with the aim of optimizing performance under static loading. The research seeks to characterize failure modes, crack patterns, and load–slip behavior under monotonic loading, with particular emphasis on the ultimate shear resistance of each pocket size to inform design guidelines for FDPC deck panel systems. The findings are expected to demonstrate potential improvements in shear capacity and ductility achieved by varying the number of large studs within UHPC-filled shear pockets confined by angle rings. However, the direct influence of angle ring confinement was not explicitly addressed in this study, as comparative results with conventional grout-filled shear pockets are still required. Ultimately, the outcomes of this research provide a foundation for future investigations, including fatigue performance, long-term durability, full-scale load testing, and parametric studies using numerical analysis, all of which are necessary to establish comprehensive and standardized design guidelines.

2 Materials and methods

2.1 *Specimens*

Eight push-off specimens were cast in L-shape, which included a bridge deck part combined with a shear pocket. The dimensions of the specimen were summarized in Table 1. The L-shape FDPC bridge deck panel was tested under the push-off loading condition, as shown in Figure 1, to perform composite actions between the concrete deck and the steel girder. The specimen consisted of a full depth concrete deck 600 mm (24 in) wide, 1,100 mm (44 in) long, and 200 mm (8 in) thick, with the enlarged end part of the deck about 500 mm (20 in) thick to apply load. A cluster of large-sized studs with a shank diameter of 31.75 mm (1¼ in) and 12 mm (4¾ in) high, spacing 63.5 mm (2½ in), was placed inside the shear pocket of the deck panel. The sizes of the pockets, depending on the stud arrangement, were set in a square or rectangular shape, cutting through the thickness of the deck.

The steel angle confinement was used around the shear pocket as suggested by Sriboonma [18]. It was assembled from 25 × 25 × 3-mm L-shape steel angle bars fillet welded in 45-degree cut-edge at each corner of the pocket. Two hook bars (DB12) were attached to each side of the angle to prevent initial cracks in the slab and to create bonding between the slab and the confinement. This angle ring confinement was cast to the bottom part of the concrete deck prior to UHPC filling in the shear pocket.

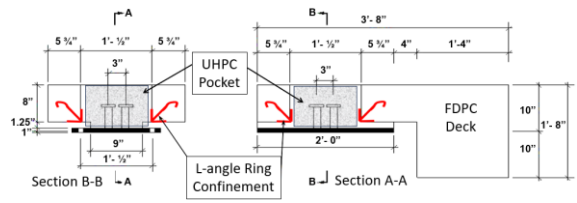

Figure 1: Geometry of the FDPC deck sample and placement of UHPC shear pocket with clustered studs.

Table 1 summarizes the 8 specimens of the push-off test. The specimens varied in three main parametric keys, including: numbers of large-sized studs, geometry, and ratios of UHPC shear pockets in terms of width and length. Four specimens were cast with the cluster of 4-studs, whereas each was set with 6- and 8-studs for two samples. In this test, four groups of UHPC pockets were considered depending on the sizing, which included a square shape of 9-inches, a

square shape of 12-inches, a rectangular shape of 9 × 12-inches, and a rectangular shape of 12 × 15-inches.

Table 1: Material properties of the push-off specimens.

Name	Numbers of Studs	Shear Pocket		Numbers of Samples
		Width (in)	Length (in)	
P-4-12-U	4	12	12	1
P-4-9-U	4	9	9	1
P-4-9x12-U	4	9	12	1
P-4-12x9-U	4	12	9	1
P-6-12-U	6	12	12	2
P-8-12x15-U	8	12	15	2

Remarks: P-A-BxC-U abbreviated as P = Push-off, A = Numbers of studs, B = Width of pocket, C = length of pocket, and U = Ultimate loading

2.2 *Fabrication*

The specimens were upside down on the ground while placing DB12 deformed bars and casting concrete, as shown in Figure 2. The blocked-out formwork was placed at the bottom part of the panel to create a void for UHPC fill-in. Ready-mixed design normal weight concrete was poured into the formwork slab and then the slabs were air curing for 28 days prior to flip-up for strain gauge installation. Meanwhile, the cluster of large-size studs was welded to the base plate as represented for a flange of steel girders of the FDPC bridge construction. The welding procedure of the studs was designed not to be a critical failure due to the welding process based on the previous study of Sriboonma [23], as well as not to fail at the shank of the studs. Figure 3 presents the cluster of large-size studs in three groups of 4-, 6-, and 8-studs. A steel base plate was punched with 10-holes throughout the thickness for bolting connection between a specimen and a steel frame in the push-off test.

After air-cured for 28 days, the decks were processed for the installation of strain gauges. The strain gauges were attached to the inner face of the angle confinement in the longitudinal and transverse directions related to the loading axis. Then, the specimens were fitted to the cluster of studs that attached to the steel plate and prepared for UHPC filling. Figure 4 presents the locations of the strain gauges installed in the angle confinement and filling mixed UHPC to the shear pocket. Each batch was individually mixed and filled in each pocket to ensure quality and volume.

Figure 2: Pre- and post-fabrication of the FDPC deck; and formworks of shear pockets with steel angle confinement.

Figure 3: Clustered large-size studs: 4, 6 and 8 studs.

Figure 4: Strain gauges installed to the angle confinement; Studs arranged in the shear pocket; and UHPC filled in the pocket.

2.3 *Material properties*

Ready mixed concrete with cylindrical compressive strength of 358 ksc (35 MPa) was used for the FDPC deck with the reinforcement of DB12 deformed bar grade SD40 (TIS) or equivalent to Grade 60 (AISC) bars. The shear pocket filled between the concrete deck and clustered studs was designed using Ultra High-Performance Concrete (UHPC). Table 2 provides the mix proportion of UHPC modified from [12]. The raw materials consisted low-carbon hydraulic cement

(TIS 2594-2556 [24]), undensified silica fume, sand (particle sizes ranging from 0.15 to 0.60 mm), tap water, superplasticizer (Sika ViscoCrete-819 Extra), and straight steel fiber (Dramix OL 13/.20). Figure 5 shows the steel fibers, the mixing process, and compressive strength testing of UHPC using cubic samples with size of 100 × 100 × 100 mm. The compressive strength of UHPC at 28 days was found at 121 MPa (1,234 ksc) after a moist-cured process. The splitting-tensile strength and elastic modulus of UHPC were 18.1 MPa (185 ksc) and 38.5 GPa (392,700 ksc), respectively.

Figure 5: Steel fiber; mixing of UHPC; and cubic compressive strength test.

Table 2: UHPC mix proportion.

	Cement	Silica Fume	Sand	Water	Super plasticizer	Steel Fiber
kg/m^3	900	225	1175	248	15	150
Weight ratio	1.00	0.25	1.31	0.28	0.02	0.17

Table 3: Material properties of the push-off specimens.

	Type/ Grade	Property	Ultimate Strength
Shear pocket	UHPC	Compressive Strength	121 MPa (17.55 ksi)
		Splitting-tensile strength	18.1 MPa (2.63 ksi)
		Elastic modulus	38.5 GPa (5,586 ksi)
Concrete slab	Normal Weight	Compressive Strength	35 MPa (5.09 ksi)
Reinforcement / Hook bars	Deform SD40	Yield Strength	235 MPa (34 ksi)
		Ultimate Strength	392 MPa (55 ksi)
Studs	SCM440	Yield Strength	450/590 MPa (65/85 ksi)
		Ultimate Strength	725/880 MPa (105/130 ksi)
Angle confinement	SS540	Yield Strength	235 MPa (34 ksi)
		Ultimate Strength	392 MPa (55 ksi)

SCM440 steel grade, yield strength 65/85 ksi and tensile strength of 105/130 ksi, was used for large-size studs according to Thai Industrial Standards (TIS) or equivalent to grade 1018 steel per Society of Automotive Engineers (SAE) standard. The ring confinement was fabricated using steel angle grade SS540 (TIS) or equivalent A36 (AISC), which had DB12 hook bars grade SD40 attached to all sides of the ring confinement. Table 3 summarizes all material properties used for each part of the specimen.

2.4 *Test setup*

The L-shape FDPC specimen was installed on the base support that was constrained to the solid floor by tightening the bolt-nut between the bottom plate of the shear pocket and the support. The load was applied by using the hydraulic jack attached to the main frame. Load cells and LVDTs were attached mostly in the vertical direction, where the slip occurred, where one LVDT was attached in the horizontal direction to monitor a tilt-up displacement of the specimen. The data acquisition system was connected to those devices and strain gauges to collect the applied forces, slip/tilt-up displacement, and deformation of steel confinement.

In accordance with common practice for evaluating stud shear connectors, the slip behavior was monitored since it governs composite interaction and can be represented by nonlinear load–slip models such as the Eurocode 4 hyperbolic law $V(s) = \frac{V_u \cdot s}{s_0 + s}$ where $V(s)$ is the shear force at slip s, V_u is the ultimate stud resistance, and s_0 is a slip parameter calibrated from testing (initial slip) or its recent refinements for UHPC pockets with clustered studs [25], [26]. For UHPC shear pockets with clustered studs, slip distribution becomes nonuniform due to the complexity of shear behavior in clustered stud systems and eccentricity effects within UHPC shear pockets, necessitating advanced modeling techniques Ding *et al*. [27] and Zhu *et al*. [28] to accurately predict slip and ensure structural integrity.

Figure 6 shows the front- and side-view of the push-off test set-up where the FDPC specimen was tightened to the base support. The hydraulic jack, load cell and LVDT were attached at the top of the specimen, whereas the tilt-up was measured from the transverse LVDT installed at the rear side of the specimen. Two strain gauges attached to the longitudinal and transverse confinement were then plugged into the data acquisition system, where they

collected the deformation every 0.03 seconds. Preloading was applied to the specimen to ensure the stability and fitting of the installation. This was done manually by loading 5 kN per time-step up to 50 kN and releasing it to the original position. The loads were then gradually increased again at the same rate until initial cracks were observed, which presented a yield limit. After that, the loads were continually increased until the failure occurred, which was stated as the maximum shear resistance of the shear connection.

Figure 6: Push-off test set-up (Front, Side and Back View) and Installation of load cells and LVDTs.

3 Results and Discussions

3.1 *Crack pattern and failure modes*

Cracks were observed in three stages: first lines, shear stage, and failure cracks. The first line cracks varied with the loads of 16 to 20 Ton-force and were found on the top surface of all FDPC specimens across from side-to-side in a straight line. These cracks are located at the section where the concrete enlarged end and full-depth parts of the slab were connected. The cracks occurred due to the eccentric load of the hydraulic jack, lined at the mid-section of the slab depth (about 10-in from the bottom of the slab). Noted, this behavior somehow could represent the behavior of the shear resistance of the UHPC shear pocket under the negative bending moment effect, combined with the shear capacity of the FDPC deck panel.

The second stage, as shear cracks, was initially found on the bottom siding of the deck and propagated to the top surface in a 45-degree incline plane. The load ranges of 35 to 45 Ton-force were initiated for the shear cracks on most of the specimens and expanded up to the failure stage. The ultimate loads of all specimens varied from 50 to 75 Ton-force, which caused failure cracks to be found around the bottom surface of the FDPC deck. By increasing the load, finally, cracks were propagated across the bottom width of the deck slab until concrete crushing around the shear pocket interface.

Figure 7 presents the example of the cracks pattern of P-6-12-Ua on three sides: left, right and front panel. The initial cracks normally observed at the front panel and extended to the sides because of the flexural behavior of the loading position. Shear cracks were observed at the bottom corner face on both the left and right sides of the panel and then propagated to the front panel until failure.

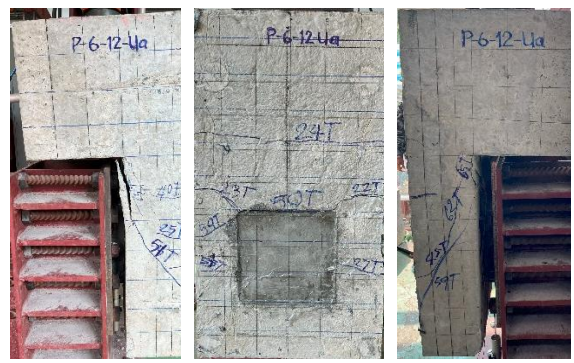

Figure 7: Crack patterns of the specimen P-6-12-Ua from the left-side, front-, and right-side-view.

Comprehensive crack maps of some different configurations of specimens: P-4-12-U, P-4-9-U, P-8-12x15-Ua, and P-4-9x12-U are presented in Table 4, which includes each face of failure, including at the closed-up interface between the FDPC slab and UHPC pockets. Most of them showed the consistent trendline of cracks as follows: At the front face, flexural cracks ran from the side across the slab toward the UHPC pocket due to eccentric loading, while shear cracks were found on the side faces only and ran from the bottom of the specimen toward the front face. UHPC pockets found no cracks, while slippages out of the shear pockets were noticed.

In addition, the UHPC shear pocket was cut to observe the orientation and distribution of the steel fiber within the pocket, since it has a significant impact on the ability of the UHPC to carry the stresses and the fiber may segregate through the depth of the shear pocket [29]. Therefore, the visual observation on the cut surfaces of the UHPC pocket was performed to characterize the distribution and alignment of the steel fibers.

Table 4: Crack patterns from different sides of push-off specimens with various UHPC configurations.

Specimen	Crack Patterns at Different Views			
	Front	Right	Left	Interface
P-4-12-U				
P-4-9-U				
P-8-12x15-Ua				
P-4-9x12-U				

Figure 8 expresses the cut and magnified surfaces of the UHPC pocket (6 studs configuration P-6-12-U) on top and side views across the longitudinal direction of loading. The image was modified with +400% color saturation and +20% brightness to differentiate the fibers from the concrete

surface. The fibers showed light distribution in the top surface, where they aligned 90 degrees in the longitudinal direction (parallel to studs). On the other hand, the fibers on the side surface showed more uniform distribution in the transverse direction across loading. For more accurate results on the distribution and orientation of the fibers, image analysis techniques may be required.

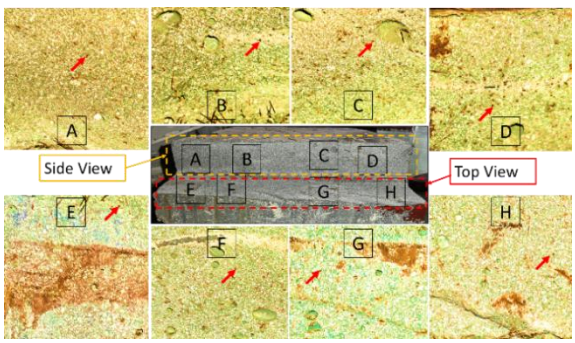

Figure 8: Fiber distribution on cut surfaces (Top and side views) of the UHPC pocket.

Table 5: Failure loads at three stages of cracks.

Specimen	Stages of Crack						
	Initial		Shearing		Failure		
	Load (T-f)	Face	Load (T-f)	Face	Load (T-f)	Face	Failure mode
P-4-12-U	20	F	57	S	60	S	FC
P-4-9-U	20/ 24	S/ F	50	S	55	S	FC & US
P-6-12-Ua	22	F	45	S	65	S	FC
P-6-12-Ub	20	F	41	S	62	S	FC
P-8-12×15-Ua	17	F&S	39	S	75	S	FC
P-8-12×15-Ub	16	S	36	S	66	S	FC
P-4-12×9-U	18	F&S	36	S	50	S	FC & US
P-4-9×12-U	13	F&S	35	S	53	S	FC &US

Note: F = Front face, S = Side face, F&S = Front and Side face
FC = FDPC crushing, US = UHPC shear cut

Table 5 summarizes the load ranges found for the crack evolution of all push-off specimens. It was found that the specimen with a square shape of the shear pocket, whether 9- or 12-inch square, could carry higher initial cracks due to negative bending than the rectangular shape pocket. This could be noticed for the initial loading of the second stage as shear cracks. The difference in loads is from 20 to 40 percent of the bottom line. However, the initial cracks did not impact the ultimate load at the failure stage, as can be seen that a cluster of 8-stud with rectangular pocket still resisted the highest load numbers.

By comparing the number of studs, a cluster of more studs resulted in an earlier cracking stage for both initial and shear cracks. The specimen P-8-12×15-Ua, which has 8-stud got initial and shear cracks at 17 and 39 Ton-force, and these are less than those of the group of 6-stud specimens P-6-12Ua by about 10 to 15 percent. This also applied to the group of specimens with 4-stud as well, P-4-12-U, which has cracking stages at 20 and 57 Ton-force for initial and shear cracks greater than both groups of 6- and 8-stud cluster specimens.

3.2 *Load-slip relationship*

Three main specimens with different numbers of clustered studs were compared in terms of load-slip relationships, including P-4-12×9-U, P-6-12-U, and P-8-12×15-U, as shown in Figure 9. The total initial slip up to 6- to 7-mm was removed from the graph due to interface contact slip under the preloading stage and due to movement at the base of the steel frame. The slip from the interface expresses only 1- to 2-mm when the hydraulic jack completely contacts the specimen, which was an inevitably low value and can be neglected. The movement at the base steel frame was measured around 5- to 6-mm due to non-flatted surface between the steel plate and the concrete floor. This can be fixed in the future by using shim plates or grout. However, the research team had measured movement of the steel frame and used this data for subtracting to the total displacement prior to evaluating the load-slip, shear capacity and ductility as detailed in the following section.

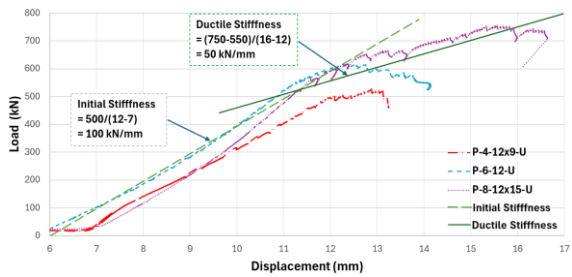

Figure 9: Relationship between load and slip of specimens with different numbers of clustered studs.

The results showed that the same trends among those three groups of specimens could be observed at the early stages of the load-slip relation. Once shear cracks occurred, a softening of ductility was found on all specimens. However, it can be noticed that more studs resulted in more ductility performance, especially after softening. At the initial stage, the specimen with 4-stud, 6-stud, and 8-stud (P-4-12×9-

U, P-6-12-U and P-8×12×15-U) could resist slippage around 6-mm prior to failure. However, after cracks, the specimen with more studs tended to sustain more ductility effects as well as higher shear capacity resistance and energy absorption before complete failure. The group of 6-stud had extended displacement to 8-mm at failure, while the specimen with 8-stud could sustain longer displacement of around 9.5 mm. This implies that using UHPC pockets with larger numbers of studs could significantly improve ductility performance in the FDPC deck system, with around 33 percent for a cluster of 6-stud and 58 percent for a cluster of 8-stud.

Furthermore, the comparative analysis of the load–displacement responses of all specimens also reveals a distinct influence of stud number on toughness, defined as the total energy absorption capacity represented by the area under the load–slip curve. The toughness of P-4-12×9-U, P-6-12-U and P-8-12×15-U, estimated from a triangular plus rectangular area under load-slip curves, equals to 2,175, 2,880, and 4,200 kN-mm, respectively. The comparative findings indicate that increasing the number of large-size studs not only improves load-carrying capacity and stiffness but also significantly enhances toughness and ductility. The 8-stud configuration provides the most reliable and resilient connection system, 93 percent higher than the group of 4-stud, suitable for applications requiring high energy absorption and structural robustness, such as in seismic or fatigue-prone environments. Conversely, the 4-stud system is prone to premature stiffness degradation and limited ductility, while the 6-stud system offers an intermediate performance level, with 32 percent higher than the 4-stud specimen.

3.3 Shear strength and stiffness

According to AASHTO LRFD Article 6.10.10 [21], the shear strength equations based on normal strength concrete were used to evaluate the shear resistance capacity of the UHPC shear pocket with clustered studs as follows:

$$P_u = \phi_{sc} 0.5 A_s \sqrt{E_c f_c'} \leq \phi_{sc} A_s f_u \quad (1)$$

where ϕ_{sc} = resistance factor for shear connectors equals to 0.85; A_s = cross-sectional area of the studs (in^2); E_c = elasticity modulus of concrete (ksi); f_c' = compressive strength of concrete cylinder (ksi); and f_u = tensile strength of the studs (ksi).

In the case of the UHPC shear pocket, the smaller strength of concrete between UHPC and FDPC was considered. For the cluster of studs, the total cross-sectional area of each stud multiplied by the number of studs was applied to Equation (1) to determine the ultimate shear capacity of the specimen.

Similarly, Eurocode 4 (EN1994-1-1 / EN1994-1-2) prescribes design resistance as the minimum of a steel limit and a concrete limit, commonly written in Equation (2).

$$P_{Rd} = min\ \left(\frac{0.8\, f_u\, A_{sc}}{\gamma_v}, \frac{0.29\, \alpha . d^2 \sqrt{E_{cm}\, f_{ck}}}{\gamma_v} \right) \quad (2)$$

where f_u = ultimate tensile strength of the studs (MPa); A_{sc} = cross-sectional area of the studs (mm^2); γ_v = Partial safety factor for shear connection to 1.25; α = aspect ratio factor = 0.2(h/d+1); h = height of stud (mm); d = shank diameter of stud (mm); E_{cm} = Secant modulus of elasticity of concrete (MPa) = 22,000×$(\frac{(f_{ck}+8)}{10})^{0.3}$; and f_{ck} = compressive strength of concrete cylinder (MPa).

Table 6 summarizes the shear strength capacity of the specimen compared to the ultimate shear strength according to AASHTO LRFD and Eurocode 4 equations. Both Equations (1) and (2) express the ultimate shear capacities governed by crushing/splitting of concrete slabs, mainly, not from UHPC or steel studs, which are presented in terms of P_U and $P_{Rd,}$ respectively. The failure loads are represented in terms of F_{test}, which consists of shear loads from the direct shear force (F_V) from the hydraulic jack and the indirect shear force (F_{Mp}) due to eccentric loading applied to the specimen. The distance of eccentric, about 8-inch, is measured from the center of the hydraulic jack to the half of full-depth of the deck concrete. Noted, the indirect shear force was determined from the flexural stresses transferred across the FDPC panel width with 1-inch stress high from the bottom of the panel and 3-inch spacing between the pair of studs.

For stiffness, similar trends were found at the elastic stage up until shear cracks occurred – then the stiffness decayed. The stiffness at the initial stage, based on comparing the peak load at the shear crack to the slippage distance, was about 10 Ton-force/mm. The researcher also found that the initial slip of all test results was not applied only to the direct displacement of the sample but also to the deformation of the base plate in the test setup. Figure 10 showed the estimated equation for stiffness evaluation of the base plate at

the corner (CH-1), mid-front (CH-2) and mid-rear (CH-3). By including this adjustment to the stiffness calculation, the final initial stiffness of all test results varied around 170 to 250 kN/mm instead.

Table 6: Comparison of shear strength per AASHTO LRFD equation versus test results.

Specimen	F_V (T-f)	F_{Mp} (T-f)	F_{test} (T-f)	n	LRFD P_u (T-f)	F_{test}/P_u	Euro code 4 P_{Rd} (T-f)	F_{test}/P_{Rd}
P-4-12-U	60	90	150	4	137	1.096	104	1.439
P-4-9-U	55	83	138	4	137	1.005	104	1.319
P-6-12-Ua	65	98	163	6	205	0.791	156	1.040
P-6-12-Ub	62	93	155	6	205	0.755	156	0.992
P-8-12×15-Ua	75	113	188	8	274	0.685	208	0.900
P-8-12×15-Ub	66	99	165	8	274	0.603	208	0.792
P-4-12×9-U	50	75	125	4	137	0.913	104	1.200
P-4-9×12-U	53	80	133	4	137	0.968	104	1.271

Note: n = Number of studs.

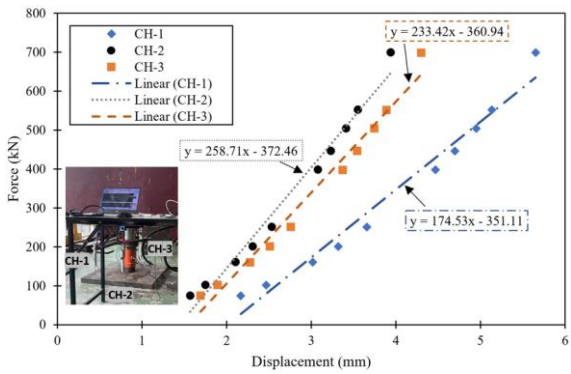

Figure 10: Stiffness of the steel base plate of the test setup at different locations (front, back and corner).

3.4 *Interface shear strength*

3.4.1 Effect of the number of studs

With the ratio comparison of the failure load to the shear resistance capacity in Table 6, the result showed that a cluster of 4-stud with a UHPC shear pocket could retain more shear transfer to the FDPC deck than those of the specimens with cluster of 6- and 8-studs. The specimens with 4-studs showed the failure load ratio in a range from 0.913 to 1.096 for LRFD and from 1.200 to 1.493 for Eurocode, which depends on the shape of the shear pocket effect.

The specimens with 6-studs, regardless of the pocket shape factor, showed a failure ratio in a range of 0.755 to 0.791 for LRFD, which implied that the other two studs added were overqualified for this system – the failure controlled by early crushing of the concrete slab at 150 Ton-force. However, the failure ratio for Eurocode was in the range of 0.992 to 1.040, which was closely matched to the load test capacity – the failure was still controlled by concrete crushing, but the secant modulus of elasticity of concrete and aspect ratio of studs played an important role in this equation.

The specimen with 8-stud and rectangular shape of pockets performed less shear capacity in a range of the failure load ratio of 0.603 to 0.685 for LRFD and 0.792 to 0.900 for Eurocode – the failure was also controlled by early crushing of the concrete slab at 165 Ton-force. The comparison of the failure ratio to LRFD showed that the cluster of 4 studs seemed to be compatible with the design equation, whereas the less effective shear resistance of the FDPC with UHPC shear pocket occurred about 20 percent for each 2-stud increment, regardless of the shape factor of the pocket. However, when compared with Eurocode 4, the failure ratio of the cluster of 6 studs was closely matched than the others, whereas the reduction of 15 percent was expected for the group of 8 studs. Noted that the Eurocode 4 equation seems to be underestimated for designing the connection for a cluster of 4 studs since the failure ratio seemed to be higher, from about 20 to 40 percent, regarding of the shape factor effect of the pocket-12 inches square shape was the most effective, whereas 12×9 inches rectangular was the lowest.

In summary, while increasing the number of studs can lead to earlier crack initiation, it generally enhances the overall ductility and ultimate displacement capacity of the connection. However, an excessive number of studs (beyond four) may lead to diminishing returns in terms of shear resistance efficiency, necessitating a reduction factor for design considerations. According to the AASHTO LRFD Equation (1), the specimens with the cluster of 4-studs in a square shape UHPC pocket showed the most dependable for designing. However, this equation was not applicable when using it with larger than 4 studs for each UHPC shear pocket. If the equation is to be

used for guidelines or determination of composite action capacity, the multiplication factor of 0.8 is recommended for each 2-stud addition per pocket. In essence, the reduction factor serves as a practical adjustment to existing design equations, making them more suitable for the unique behavior of UHPC shear pockets with a higher density of large-sized studs. On the other hand, the Eurocode Equation (2) was found to be underestimated for designing the cluster of 4 studs and more compatible when used with the group of 6 studs, therefore, the multiplication factor of 0.8 is still recommended for each pair greater than the group of 6 studs.

Noted, the multiplication factor of 0.8 was derived from empirical data as a rounded value, evaluated by dividing the average failure load by the ultimate shear resistance from the design code for each stud group. For the group with 6 studs, the ratio was 0.776 (159 T-f / 205 T-f), while for the group with 8 studs it was 0.644 (176.5 T-f / 274 T-f). Notably, the value of 0.644 approximates the square of 0.8 (0.8×0.8), which supports the recommendation of adopting 0.8 as the multiplication factor in this study, representing the incremental effect of each additional stud pair. Nevertheless, further experimental results are required to validate this factor with greater accuracy, as the value may fall below 0.8, as observed in the 4-stud case (0.776), which differs by approximately 3%.

3.4.2 Effect of UHPC material

From Table 4, the shear resistance capacity of the FDPC deck system was considered from three main factors: crushing of the deck (P_{conc}), crushing of the UHPC pocket (P_{UHPC}), and tearing of the studs(P_{steel}). The failure mode observed by all specimens showed that the main factor that controlled the ultimate resistance was the concrete strength of the FDPC deck. Therefore, a smaller width of a shear pocket could be justified when using UHPC materials.

To observe the effectiveness of UHPC materials, the specimens with different pocket widths were compared. With the same number of studs, the specimen P-4-12-U tended to sustain ultimate shear resistance (150 T-f) more than that of the specimen with a smaller width of the UHPC pocket, as P-4-9-U (138 T-f), for about 8.7 percent. However, the result showed in the opposite direction when comparing P-4-12×9-U and P-4-9×12-U. The smaller width of the UHPC pocket P-4-9x12-U could sustain more failure load than the one with 12-inch width of the pocket P-4-12×9-U, about 6.4 percent, which correlated to the assumption mentioned earlier.

Nonetheless, after removing UHPC shear pockets from the FDPC panel, plain shear cuts at the top of the clustered studs were observed mostly on the pocket of the specimen with 4-stud, except P-4-12-U with the 12-inches width square pocket as shown in Figure 11. This implied that even UHPC materials, which have higher ductility than NSC, the edge or clear covering of the large-size studs still played an important role in the design consideration. To gain the most composite action transferring against the FDPC panel to the UHPC pocket, the minimum edge distance or clear covering of studs shall not be less than 3-times of the diameter of studs.

It can be noticed that no shear cut failure of UHPC pockets was found on the pockets sized larger than 12 inches in width, except the specimen with 8-studs P-8-12x15-Ua, which signed some fractures along the top level of the clustered studs. This might be evidence that steel fibers inside UHPC could long the crack failure of the FDPC panel system.

Figure 11: Internal section and shear cut failure of UHPC shear pocket.

3.4.3 Effect of UHPC pocket geometry

Among the specimens with 4-stud, the most effective shear resistance was found in the specimens with a square shape pocket, either 12-inches or 9-inches wide. Even though the specimen with a 9-inches square width pocket could sustain a smaller shear (around 8%) than that with a 12-inches pocket, the failure load ratio was still higher than the computation from the AASHTO LRFD equation, as seen from Table 4. On the other hand, the specimen with a

rectangular pocket (P-4-12×9-U and P-4-9×12-U) gave a smaller load failure ratio (from 3.6% to 9.4%) than that of the specimen with a 9-inches square width, regardless of the pocket layout.

When comparing the specimen with the rectangular pocket with different layout angles, the higher load failure ratio was found in the specimen with a smaller UHPC width section (P-4-9×12-U). The effect took about 6.4 percent with the aspect rectangular ratio of 0.75 (9 to 12 inches). The researchers believe that this effect will develop more when a less aspect ratio of the pocket takes place. The geometry of the shear pocket, including its shape (square preferred over rectangular for efficiency) and width, along with the number and precise arrangement of large-sized studs, are critical factors that dictate the overall shear resistance capacity of the connection. Designs must account for these geometric effects to ensure reliable performance.

4 Conclusions

The push-off test was conducted with 8 FDPC specimens with a cluster of large-size studs in a UHPC shear pocket. The variable parameters for this study consisted of numbers of studs and aspect ratios in terms of pocket sizing and layout were considered for studying the behavior of this system in terms of strength, slippage, stiffness, crack patterns and failure modes. Based on the experiment, three crack patterns were detected: initial cracks on the front panel due to flexure from eccentric loading in the test setup, shear cracks propagated on the side of the panel, and failure cracks from concrete crushing of the FDPC interface to the UHPC pocket. Two failure modes existed due to concrete crushing on the FDPC interface for all specimens, and the shear plain cut of the UHPC pockets at the top layer of the studs. The second failure mode was found only on the specimens with 4-studs in the 9-inches UHPC pockets. By comparison of the failure load ratio between the test loads and the AASHTO LRFD shear resistance equations, the specimen with 4-studs showed the most effective for utilizing with the FDPC bridge deck panel system. The specimens with 6- and 8-studs showed less shear resistance than the equation and required a multiplication reduction factor of 0.8 applied for each stud pair increments to evaluate a suitable shear resistance capacity for this system. Compared with Eurocode 4, the specimen with 6-studs was found to be more compatible than the specimen with 4-stud, which seemed to be underestimated by about 20-40 percent. The specimen with 8-studs showed an overestimate of about 20 percent, therefore, a reduction factor of 0.8 is still suggested for each pair increments more than 6-studs for the Eurocode equation. The specimen with a square shape of the UHPC pocket tended to sustain more effective shear resistance than those with a rectangular shape, from 3.6 to 9.4 percent. In contrast, the specimen with a 12-inches square shape tended to resist more shear load than that of the specimen with a 9-inches square shape pocket, about 8 percent. The layout of the rectangular shear pocket has impacted on the shear resistance capacity. The higher load failure ratio was found in the specimen with a smaller UHPC width section P-4-9×12-U than the specimen P-4-12×9-U, about 6.4 percent. The researcher believes that, by comparing per individual stud, using UHPC pockets with a cluster of 4-large studs is the most advantageous for the FDPC deck system, regardless of the pocket shape factor, even though the total shear resistance and ductility may be less than that of a cluster of 6- and 8-studs. Nevertheless, larger numbers of over 4 large studs can be utilized whenever rapid construction and replacement processes are needed. In conclusion, these findings highlight the need for design adjustments to existing codes when utilizing UHPC shear pockets with large-sized stud clusters, emphasizing the importance of specific reduction factors, optimal stud configurations, and careful consideration of pocket geometry and material interactions to ensure robust and ductile bridge deck systems. However, for long-term performance of the bridge application, further studies regarding the effects of fatigue, creep and shrinkage shall be included for design consideration.

Acknowledgments

This research was funded by King Mongkut's University of Technology North Bangkok, Contract no. KMUTNB-68-BASIC-11. The authors would like to express gratitude to all staff involved in this research including the faculty of technical education and the college of Industrial Technology.

Author Contributions

K.S.: conceptualization, methodology, research design, data analysis, investigation, writing-original draft, funding acquisition and project administration;

N.K.: conceptualization, methodology, research design, data analysis, investigation, writing-reviewing and editing, and supervision; K.C., K.R.: writing-reviewing and editing. All authors have read and agreed to the published version of the manuscript.

Conflicts of Interest

The authors declare no conflict of interest, no known competing financial interests or personal relationships that could have appeared to influence the work reported in this paper.

Declaration of generative AI and AI-assisted technologies in the writing process

The authors utilized the ChatGPT tool to enhance the language and readability of the manuscript.

References

[1] K. E. Hanna, G. Morcous, and M. K. Tadros, "Rapid construction of Pacific Street Bridge," *SPR-PL-1 (037) P587*, 2010.

[2] K. E. Hanna, G. Morcous, and M. K. Tadros, "Standardized precast prestressed concrete panels for bridge decks," in *Proceedings of the Concrete Bridge Conference*, 2008.

[3] F. Menkulasi and C. L. Roberts-Wollmann, "Behavior of horizontal shear connections for full-depth precast concrete bridge decks on prestressed I-girders," *PCI Journal*, vol. 50, no. 3, pp. 60–73, 2005.

[4] S. S. Badie, A. F. M. Girgis, M. K. Tadros, and K. Sriboonma, "Full-Scale testing for composite slab/beam systems made with extended stud spacing," *American Society of Civil Engineers (ASCE), Journal of Bridge Engineering*, vol. 16, no. 5, pp. 653–661, 2011.

[5] M. A. Issa, J. S. Salas, H. I. Shabila, and R. Z. Alrousan, "Composite behavior of full-depth precast slabs installed on precast prestressed girders," *PCI Journal*, vol. 51, no. 5, pp. 132–145, 2006.

[6] K. Sriboonma and S. S. Badie, "Practical steel confinements for widely spaced clustered large stud shear connectors in composite bridge deck panel systems," in *Proceedings of the Steel Conference and Structures Congress (NASCC)*, Florida, USA, May 12–15, 2010.

[7] *ASTM C1856-17: Standard Practice for Fabricating and Testing Specimens of Ultra-High Performance Concrete*, ASTM International, West Conshohocken, PA, USA, 2017.

[8] B. A. Graybeal, "Material property characterization of ultra-high performance concrete," *FHWA-HRT-06-103*, Federal Highway Administration, McLean, VA, USA, Aug. 2006.

[9] Z. Fang, H. Jiang, J. Xiao, X. Dong, and T. Shao, "Shear performance of UHPC-filled pocket connection between precast UHPC girders and full-depth precast concrete slabs," *Structures*, vol. 29, pp. 328–338, Feb. 2021.

[10] J. Q. Wang, J. N. Qi, T. Tong, Q. Z. Xu, and H. L. Xiu, "Static behavior of large stud shear connectors in steel–UHPC composite structures," *Engineering Structures*, vol. 178, pp. 534–542, 2019.

[11] C. Muñoz, A. Miguel, D. K. Harris, T. M. Ahlborn, and D. C. Froster, "Bond performance between ultrahigh-performance concrete and normal-strength concrete," *Journal of Materials in Civil Engineering*, vol. 26, no. 8, p. 04014031, 2014.

[12] P. Wongtala, N. Chaimoon, N. Khomwan, and K. Chaimoon, "Experimental and numerical study on structural behavior of reactive powder concrete corbels without stirrups," *Case Studies in Construction Materials*, vol. 19, p. e02372, 2023.

[13] M. Al-Rousan, R. Hasan, and Y. Al-Rimawi, "The influence of prestress level on the behavior of prefabricated full-depth precast bridge decks," *Case Studies in Construction Materials*, vol. 19, p. e02307, 2023, doi: 10.1016/j.cscm.2023.e02307.

[14] Z. Xiong, L. Feng, Y. Zou, X. Wang, and W. Huang, "Experimental study of high-strength steel–precast prestressed concrete composite beams under hogging moment," *Journal of Constructional Steel Research*, vol. 211, 2024, Art. no. 108784, doi: 10.1016/j.jcsr.2024.108784.

[15] G. Wang, B. Xian, F. Ma, and S. Fang, "Shear performance of prefabricated steel–UHPC connections," *Buildings*, vol. 14, no. 8, 2024, Art. no 2425, doi: 10.3390/buildings14082425.

[16] A. Stefaniuk, A. Bąk, and K. Flaga, "Full-scale testing of UHPC deck systems with studs in shear pockets," *Engineering Structures*, vol. 301, 2024, Art. no. 117339, doi: 10.1016/j.engstruct.2024.117339.

[17] Y. Jiang, S. Fang, F. Ma, and B. Xian, "Shear performance of headless studs in UHPC," *Frontiers in Materials*, vol. 11, 2024, Art. no. 1451240, doi: 10.3389/fmats.2024.1451240.

[18] K. Sriboonma and S. Pornpeerakeat, "Experimental investigation of steel confinement of clustered large-size stud shear connector in full-depth precast bridge deck panel," *Key Engineering Materials*, vol. 856, pp. 99–105, Aug. 2020.

[19] K. Sriboonma, "Fatigue behavior of steel ring confinement for a clustered stud shear connector in full-depth precast concrete bridge deck panel," *Materials Today: Proceedings*, vol. 52, pp. 2555–2561, Jan. 2022.

[20] S. T. Smith and J. G. Teng, "FRP-strengthened RC beams. I: Review of debonding strength models," *Engineering Structures*, vol. 24, no. 4, pp. 385–395, 2002.

[21] *American Association of State Highway and Transportation Officials (AASHTO), LRFD Bridge Design Specifications*, 6th ed., Washington, DC: U.S. Dept. of Transportation, 2015.

[22] *EN 1994-1-2: Eurocode 4: Design of Composite Steel and Concrete Structures*, 2005.

[23] K. Sriboonma, "Effects of fillet weld to large-size stud shear connector in full-depth precast bridge deck panel," *Materials Today: Proceedings*, vol. 52, pt. 5, pp. 2548–2554, 2022.

[24] *TIS 2594-2567: Hydraulic Cement*, Thai Industrial Standard, Thailand, 2024.

[25] F. Qin, Z. Huang, Z. Zheng, Y. Chou, Y. Zou, and J. Di, "Analytical model for the load-slip relationship of bearing-shear connectors," *Frontiers in Materials*, vol. 10, Feb. 2023, Art. no. 1110232, doi: 10.3389/fmats.2023.1110232.

[26] K. Peng, L. Liu, F. Wu, R. Wang, S. Lei, and X. Zhang, "Experimental and numerical analyses of stud shear connectors in steel-SFRCC composite beams," *Materials*, vol. 15, no. 13, p. 4665, Jul. 2022, doi: 10.3390/ma15134665.

[27] J. Ding, J. Zhu, J. Kang, and X. Wang, "Experimental study on grouped stud shear connectors in precast steel-UHPC composite bridge," *Engineering Structures*, vol. 242, 2021, Art. no. 112479, doi: 10.1016/j.engstruct.2021.112479.

[28] Y. Zhu, W. Z. Taffese, and G. Chen, "Data-driven shear capacity prediction of studs embedded in UHPC for steel–UHPC composite structures," *Journal of Structural Engineering*, vol. 151, no. 9, 2025, Art. no. 04025119, doi: 10.1061/JSENDH.STENG-13818.

[29] E. (Nadelman) Wagner and J. S. Lawler, "Evaluation of fiber distribution and alignment in structural UHPC elements," *International Interactive Symposium on Ultra-High Performance Concrete Papers*, vol. 2, no. 1, Jun. 2019.